

# Image Smoothing with Savitzky-Golay Filters

Srinivasan Rajagopalan, Richard Robb  
Mayo Clinic and Foundation

## ABSTRACT

Noise in medical images is common. It occurs during the image formation, recording, transmission, and subsequent image processing. Image smoothing attempts to locally preprocess these images primarily to suppress image noise by making use of the redundancy in the image data. One-dimensional Savitzky-Golay filtering provides smoothing without loss of resolution by assuming that the distant points have significant redundancy. This redundancy is exploited to reduce the noise level. Using this assumed redundancy, the underlying function is locally fitted by a polynomial whose coefficients are data independent and hence can be calculated in advance. Geometric representations of data as patches and surfaces have been used in volumetric modeling and reconstruction. Similar representations could also be used in image smoothing. This paper shows the two and three-dimensional extensions of one-dimensional Savitzky-Golay filters. The idea is to fit a two/three-dimensional polynomial to a two/three-dimensional sub region of the image. As in the one-dimensional case, the coefficients of the polynomial are computed a priori with a linear filter. The filter coefficients preserve higher moments. The coefficients always have a central positive lobe with smaller outlying corrections of both positive and negative magnitudes. To show the efficacy of this smoothing, it is used in-line with volume rendering while computing the sampling points and the gradient.

**Keywords:** image preprocessing, smoothing, edge preservation, linear filters, Savitzky-Golay filters, anisotropic diffusion, volume rendering, raycasting, splatting.

## 1. INTRODUCTION

The maximum potential of multi-dimensional biomedical images lies not in merely acquiring them but in unraveling the rich information they contain for practical use [1]. However, the fidelity of medical images is invariably deteriorated by noise due to interference and other phenomena that affect the measurement process. In addition, the subsequent recording and transmission might also contribute to information loss. The quest to effectively analyze biomedical images and comprehend their information content so as to precisely quantify and interpret the structure and function of the imaged object begins with image enhancement. Image enhancement techniques attempt to improve the quality of an image for further processing like segmentation, registration, visualization, mensuration etc. Suppressing the noise in an image by smoothing is one of the common image enhancement strategies. There is however, a tradeoff between the level of detail and noise reduction. To strike a meaningful balance between the two, significant efforts have been directed towards both linear and nonlinear smoothing techniques. In this paper, we present the use of a linear filter based on the extension of one-dimensional Savitzky-Golay filters [2] to smooth two and three-dimensional images. This filtering is incorporated into the volume rendering pipeline for smoothing the results of point resampling and gradient computations. While some other classical smoothing approaches might be effective for generally smoothing a volumetric dataset, they might not be amenable during the process of raycasting or splatting, and hence become untenable.

## 2. SMOOTHING OPERATIONS

Smoothing algorithms can be broadly grouped under linear and non-linear categories. Linear algorithms typically involve calculating the new value of a pixel  $p(i, j)$  based on a linear weighting of brightness values in a local neighborhood  $N$ . This can be represented mathematically as

$$p(i, j) = \sum_{m \in N} \sum_{n \in N} weights(i - m, j - n) o(i, j) \quad (1)$$

where  $p$  and  $o$  represent the processed and original image respectively and  $weights$  represent the linear weighting. Equation (1) is equivalent to discrete convolution and the  $weights$  can be referred to as *convolution mask*. The region of support can be either rectangular or circular. By suitably selecting the *mask*, various filters can be realized. Figure 1 shows the 5x5 *masks* for some typical filters.

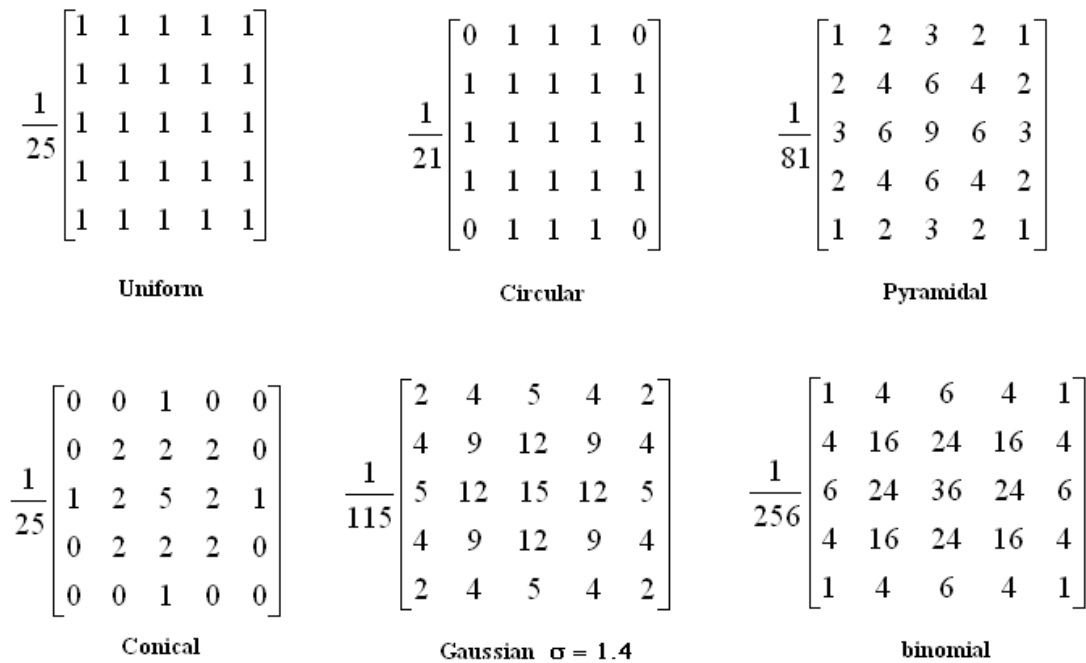


Figure 1: Convolution masks for some linear filters

Since smoothing attempts to suppress minor fluctuations in the image, it is equivalent to suppressing high frequency components in the Fourier transform domain. It is possible to analyze the noise suppression characteristics of linear filters by examining their frequency response. Figure 2 shows the frequency response of the filters shown in Figure 1. It is clear from the figure that the uniform filter does not suppress high frequency components as effectively as the binomial or gaussian filters.

Linear filters perform well under the assumption that a pixel looks similar to its neighbors and that there are no changes in the gray-levels of the underlying image data. Brute-force averaging violates this assumption along the edges, leading to edge blurring. To preserve edges, a number of non-linear smoothing techniques have been proposed. This includes, but is not limited to, mean filtering [3], median filtering [4], rotating mask [5], inverse gradients [6], anisotropic

diffusion via PDE [7], multi-channel anisotropic diffusion [8], tensor non-linear anisotropic diffusion [9], and curve evolution [10]. Detailed analysis of these non-linear filters and especially those belonging to the diffusion category is given in [11].

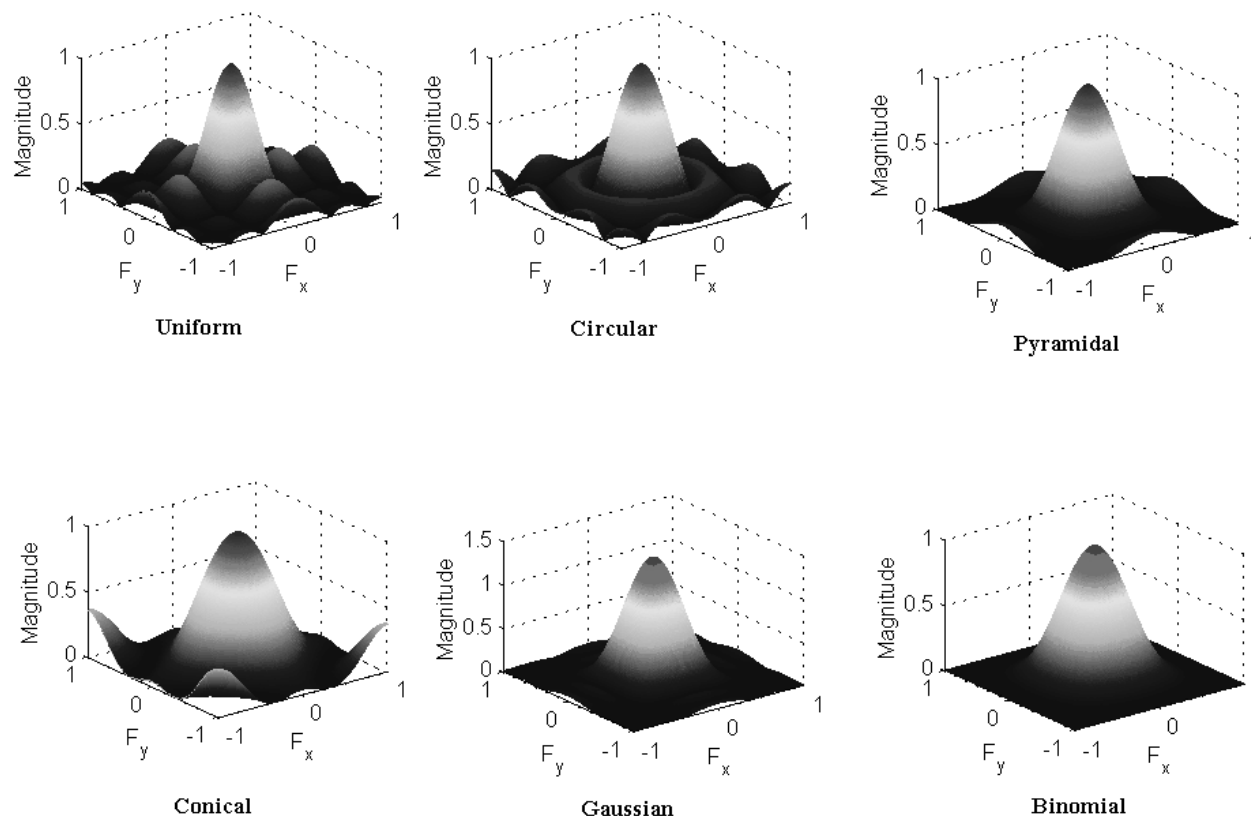


Figure 2: Frequency response of linear filters shown in Figure 1

### 3. SAVITZKY-GOLAY SMOOTHING FILTERS

The basic idea behind one-dimensional Savitzky-Golay filtering is to find filter coefficients that preserve higher moments [12]. This is done by approximating the underlying function with a polynomial of higher order. For each point in the image, a polynomial is fit to all its neighbors. The polynomial coefficients can be calculated a priori independent of the underlying data. This results in a linear filter that can be convolved with the data to effect the smoothing.

In the case of two/three-dimensional smoothing, the idea is to fit a two/three-dimensional polynomial to a two/three-dimensional sub region of the image/volume. The methodology for fitting the polynomial is given in [13]. For purpose of completion, we will show the procedure for computing the filter coefficients for a two-dimensional image with a 3x3 patch. Suppose, we want to fit a two-dimensional polynomial of order two to this data. The image patch is formed as shown in Figure 3. The corresponding polynomial is of the form

$$b(l) = p(i, j) = c_{00} + c_{10}x_i + c_{20}x_i^2 + c_{01}y_j + c_{11}x_i y_j + c_{02}y_j^2 \quad (2)$$

where  $i, j = -1:1$ ;  $l = 0:8$ ;  $p(i, j)$  represents the pixel intensity at location  $(i, j)$  and  $(x_i, y_j)$  is the pixel coordinate of  $b(l)$

		$x_i$		
		-1	0	1
$y_j$	-1	$b(0)$	$b(1)$	$b(2)$
	0	$b(3)$	$b(4)$	$b(5)$
	1	$b(6)$	$b(7)$	$b(8)$

Figure 3: Illustration of a 3x3 image patch

Equation (2) can be rewritten as

$$Xc = b \quad (3)$$

where

$$X = \begin{bmatrix} 1 & x_0 & x_0^2 & y_0 & x_0 y_0 & y_0^2 \\ 1 & x_1 & x_1^2 & y_1 & x_1 y_1 & y_1^2 \\ 1 & x_2 & x_2^2 & y_2 & x_2 y_2 & y_2^2 \\ \vdots & \vdots & \vdots & \vdots & \vdots & \vdots \\ 1 & x_9 & x_9^2 & y_9 & x_9 y_9 & y_9^2 \end{bmatrix}$$

and  $c = (c_{00} \ c_{10} \ c_{20} \ c_{01} \ c_{11} \ c_{02})^T$

From equation (3),  $c = (X^T X)^{-1} X^T b$ , where  $(X^T X)^{-1} X^T$  is the pseudo-inverse of  $X$  and is independent of the image data. The result of this pseudo-inverse could be rearranged into a traditional filter of the same size as that of the image patch. To compute the smoothed value of the pixel, the polynomial in equation (2) is evaluated at  $(x, y) = (0, 0)$ . This turns out to be  $c_{00}$ , which can be computed by applying the filter formed from the first row of the pseudo-inverse to the image patch. Similarly equation (2) could be used to compute the partial derivatives on the patch. Figure 4 shows the *convolution masks* for a 3x3 and 5x5 patch for a polynomials of order 2 and 3 respectively. Figure 5 shows the *convolution mask* for a 3x3x3 sub volume for a polynomial of order 2.

$$\begin{array}{c} \frac{1}{9} \begin{bmatrix} -1 & 2 & -1 \\ 2 & 5 & 2 \\ -1 & 2 & -1 \end{bmatrix} \\ \text{order 2} \end{array} \quad \begin{array}{c} \begin{bmatrix} -0.0743 & 0.0114 & 0.0400 & 0.0114 & -0.0743 \\ 0.0114 & 0.0971 & 0.1257 & 0.0971 & 0.0114 \\ 0.04 & 0.1257 & 0.1543 & 0.1257 & 0.04 \\ 0.0114 & 0.0971 & 0.1257 & 0.0971 & 0.0114 \\ -0.0743 & 0.0114 & 0.04 & 0.0114 & -0.0743 \end{bmatrix} \\ \text{order 3} \end{array}$$

Figure 4: Convolution mask for 2D 3x3 and 5x5 Savitzky-Golay Filter

$$\begin{bmatrix} -0.074 & 0.037 & -0.074 \\ 0.037 & 0.148 & 0.037 \\ -0.074 & 0.037 & -0.074 \end{bmatrix} \begin{bmatrix} 0.037 & 0.148 & 0.037 \\ 0.148 & \underline{0.259} & 0.148 \\ 0.037 & 0.148 & 0.037 \end{bmatrix} \begin{bmatrix} -0.074 & 0.037 & -0.074 \\ 0.037 & 0.148 & 0.037 \\ -0.074 & 0.037 & -0.074 \end{bmatrix}$$

Figure 5: Convolution mask for 2nd order 3x3x3 Savitzky-Golay filter

Figure 6 shows representative sections of the T1-weighted MRI image obtained from MNI's simulated brain database [14]. Three percent noise was included in the parameter settings. Figure 7 shows the result of applying a 3<sup>rd</sup> order 5x5 Savitzky-Golay filter on these images. Figure 8 shows the result for a 2<sup>nd</sup> order 3x3x3 filter.

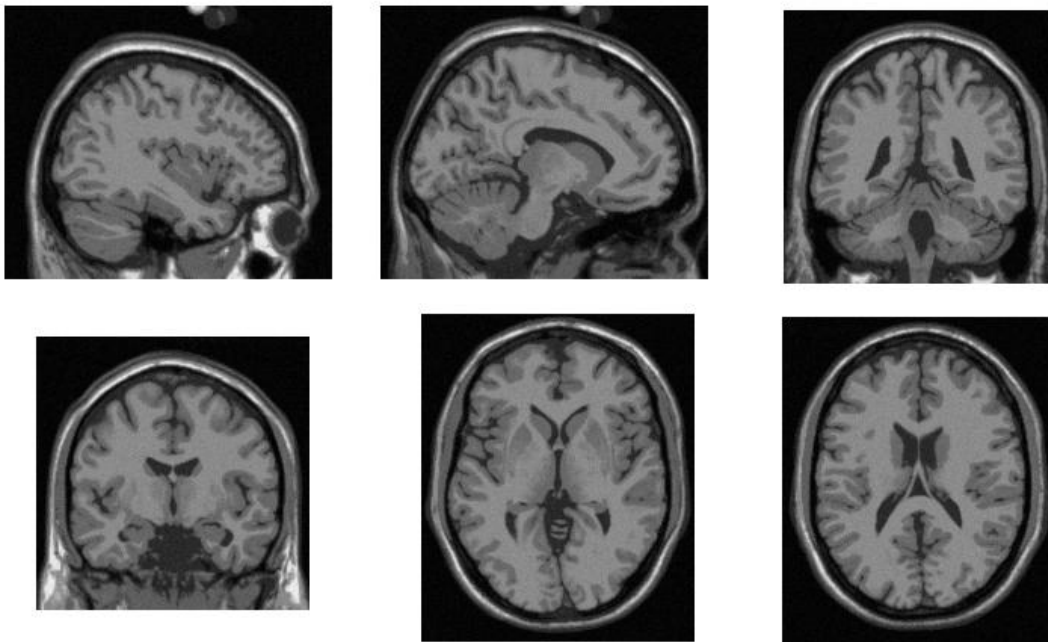


Figure 6: Selected slices from 3% noise T1 MNI normal brain

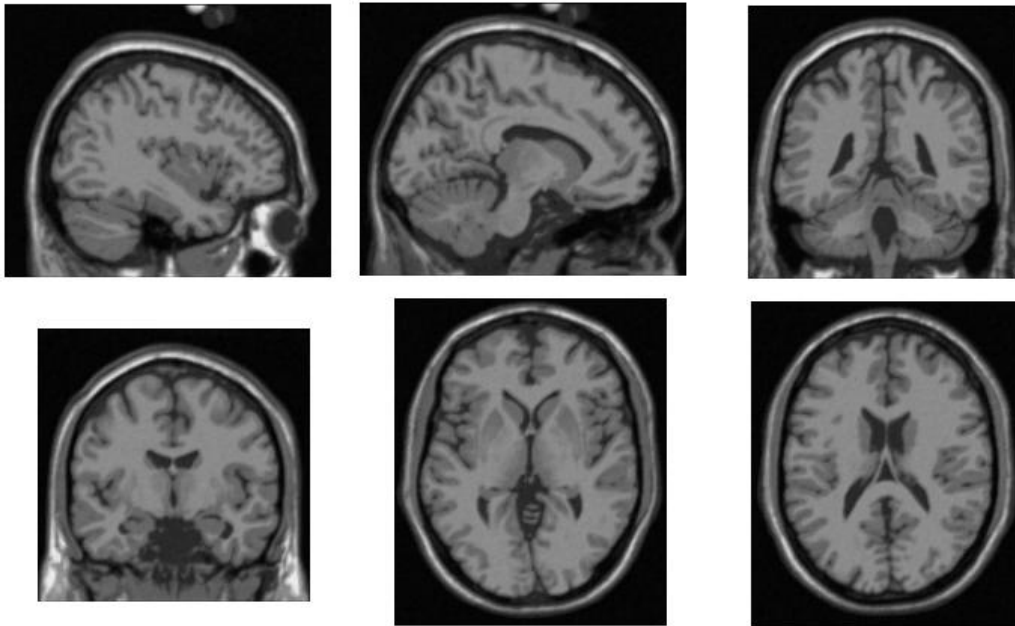


Figure 7: 3rd order 5x5 Savitzky-Golay filtering of images in Figure 6

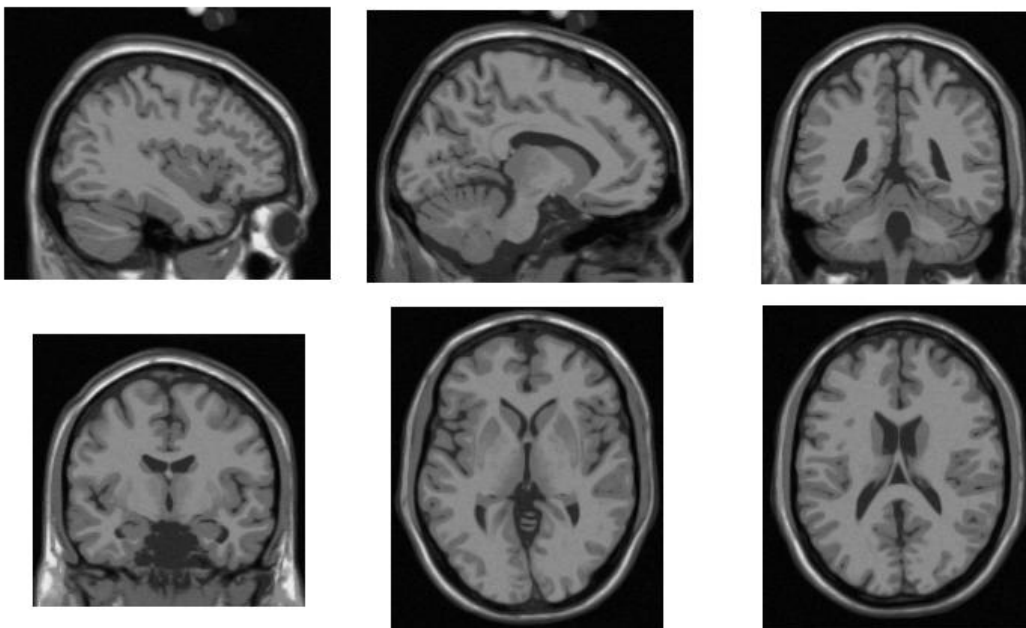


Figure 8: 2nd order 3x3 Savitzky-Golay filtering of images in Figure 6

There are noticeable differences even between the original and 2D smoothed image. Three-dimensional smoothing has further improved the results. Towards understanding these results better, Figure 9 shows the line profile for the results on the 80<sup>th</sup> sagittal section (2<sup>nd</sup> panel in Figures 6 through 8) of the MNI brain. It clearly shows the smoothing effects of 3D Savitzky-Golay filters. The results are very comparable to the non-linear smoothing based on anisotropic diffusion implemented using a variant of [7].

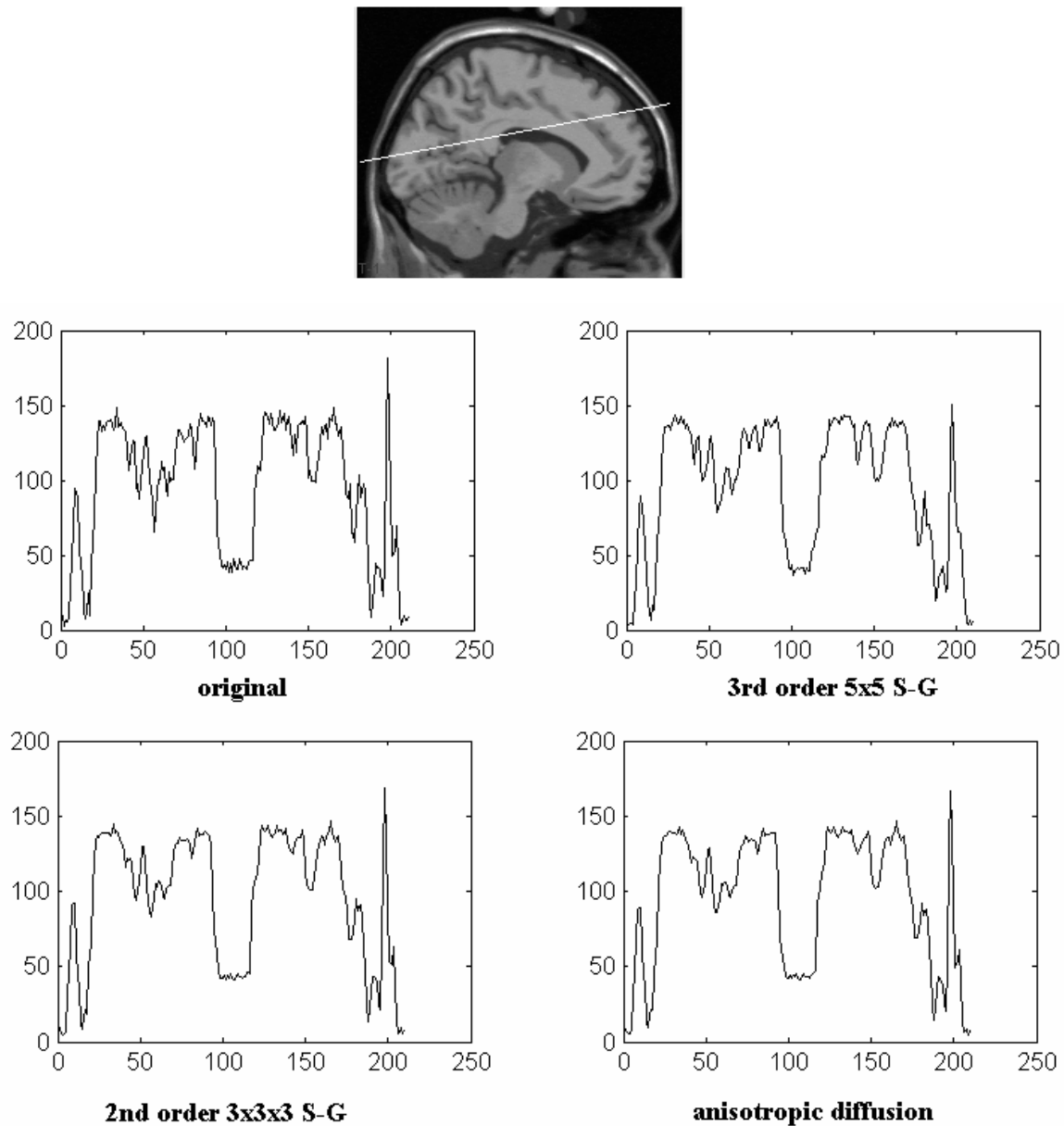


Figure 9: Profile map of S-G and anisotropic diffusion filters

#### 4. EMBEDDING SMOOTHING IN VOLUME RENDERING

Volume rendering facilitates simultaneous visualization of multiple surfaces in a volumetric dataset that represents a discrete model of an inherently continuous three-dimensional scene. The image is generated by integrating a transport function through the volume [15]. This process involves, among other steps, the resampling of voxels along the viewing rays for image space methods like ray-casting and along the projection plane for object space methods like splatting and texture mapping. This resampling step is subject to interpolation artifacts and tends to introduce spurious surfaces. The interpolation of gradients computed to shade and light the surfaces also adds to the artifacts. Furthermore, if one were to embed deformation into the visualization loop, as in [16], it would be prudent to apply local smoothing to avoid these anomalies. Though non-linear smoothing methods like anisotropic diffusion produce better results, it is not practical to use them inside the visualization loop where major but not all regions of the volume are resampled for every viewing angle and deformation step. Moreover, if one were to use volume modeling with spatial data structures like octrees to capture and render the volumetric space, it would be difficult to use scale space methods. However, linear smoothing filters like Savitzky-Golay filters can be easily incorporated under all these conditions to improve resampling and gradient computations. To illustrate this, we smoothed the sample points and gradients “on the fly” using the three-dimensional filter shown in Figure 5. Figure 10 shows the effect of smoothing on the renderings. The result on the left is without smooth resampling while that on the right has been smoothed. The improved detail provided by this simple processing is evident. The effect of smoothing under deformation will be more dramatic [16].

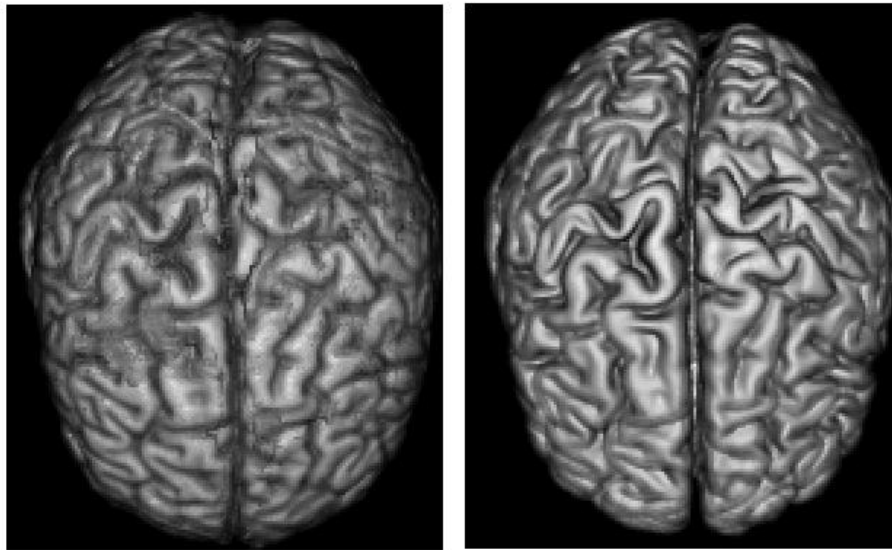


Figure 10: Effect of smoothing on volume rendering

#### 5. CONCLUSION

We have presented some insight into using Savitzky-Golay filters to smooth two and three-dimensional medical images. Like their one-dimensional counterpart, the filter coefficients depend on the polynomial order used in the least-square fitting and the window size and is independent of the underlying data. They provide good smoothing without loss of resolution. Like other local, linear smoothing filters, they can be used “on the fly” to reduce resampling and gradient computation errors during volume deformation and visualization. More study is required to evaluate the influence of polynomial order and window size on the image smoothness.



## 6. REFERENCES

- [1] Robb, R.A. *Biomedical Imaging, Visualization and Analysis*. Wiley-Liss, 2000.
- [2] Savitzky A., and Golay M.J.E. *Analytical Chemistry* vol 36:1627-1639, 1964.
- [3] Tyan S.G. Median filtering, deterministic properties. In T.S.Huang, editor, *Two-Dimensional Digital Signal Processing*, volume II. Springer Verlag, 1981.
- [4] Nagao M, and Matsuyama T. *A Structural Analysis of Complex Aerial Photographs*. Plenum Press, 1980.
- [5] Pitas I., and Venetsanopoulos A.N. *Nonlinear Digital Filters: Principles and Applications*. Kluwer, 1990.
- [6] Wang D.C.C., and Vagnucci A.H., Gradient inverse weighting smoothing schema and the evaluation of its performance. *Computer Graphics and Image Processing*. 15,1981.
- [7] Perona P, Malik J. Scale-space and edge detection using anisotropic diffusion. *IEEE Trans. Pattern Anal. Machine Intell.*, 12(7):629–639, July 1990.
- [8] Gerig G., Kubler O., Kikinis R., and Jolesz F.A., Nonlinear anisotropic filtering of MRI data, *IEEE Trans. Medical Imaging*. 11(2):221-232, 1992.
- [9] Weickert, J. *Anisotropic Diffusion in Image Processing*, Teubner-Verlag, 1998.
- [10] Sarti A., Ortiz C., Locket S., and Malladi R.A., Geometric Model for 3-D Confocal Image Analysis, *IEEE Trans on Biomedical Engineering*. 47(12):1600-1609, Dec 2000.
- [11] Suri J.S, Gao J., Singh S., and Swamy L. A Comparison of State-of-the-Art Diffusion Imaging Techniques for Smoothing Medical/Non-Medical Image Data. In Proc XV Intn'l Conference on Pattern Recognition, August 2002.
- [12] Press W.H., Teukolsky S.A., Vetterling W.T., and Flannery B.P., *Numerical Recipes in C*. Cambridge University Press. 2000.
- [13] <http://research.microsoft.com/~jckrumm/SavGol/SavGol.htm>
- [14] <http://www.bic.mni.mcgill.ca/brainweb/>
- [15] Kruger W. Volume Rendering and data feature enhancement. *Computer Graphics*. 24(5):21-26, Nov 1990.
- [16] Shiao-fen Fang, Rajagopalan Srinivasan, Raghu Raghavan, Joan Richtsmeier, "Volume Morphing and Rendering—an Integrated Approach", *Journal of Computer Aided Geometric Design*, 17(1):59-81, November 1999.